CHAPTER 4

DESIGN, ANALYSIS AND SIMULATION STUDY OF DIELECTRIC FILLED S-BAND TAPERED MAGNETICALLY INSULATED LINE OSCILLATOR (MILO)*

4.1 Outline

4.2 Introduction

4.3 Analysis

4.4 Device Modelling

4.5 Results and discussion

4.5.1 Cathode Misalignment Effect

4.6 Conclusion

*Part of this work has been published as:

Nisheeth Upadhyay, Arjun Kumar, Prabhakar Tripathi and Smrity Dwivedi "Design, Analysis and Simulation Study of Partially Dielectric Filled S-Band Tapered Magnetically Insulated Line Oscillator (MILO)," *INTERNATIONAL JOURNAL OF MICROWAVE AND OPTICAL TECHNOLOGY,* vol. 17, no. 3, pp. 234-242, May 2022.

4.1 Outline

To increase the overall efficiency of the MILO device, an S-band tapered magnetically insulated line oscillator (MILO) with partly dielectric loaded cavities is presented in this chapter. The tapered interaction cavities of the MILO are partially filled with the low loss dielectric material in the proposed structure. To determine the dispersion characteristic of the proposed MILO's resonating structure, an equivalent circuit analysis is used. Using a 3D EM simulation tool, an extensive simulation analysis is carried out to determine the electromagnetic (EM) and radio frequency (RF) behaviour of the proposed structure (i.e., CST Studio Suite). The CST's EIGENMODE solver is used to get the resonant structure's dispersion characteristics, which are also used to validate the device design parameters. CST's particle-in-cell (PIC) solver is used to examine the RF behaviour of the proposed structure with and without dielectric loading. The modelled structure is simulated with 500 kV diode voltage and 35 kA diode current. Without dielectric loading, the PIC simulation estimates that the modelled device outputs 2.4 GW average power in TM01 mode at 2.65 GHz with an electronic efficiency of 13.71 per cent. The modelled device generates an average power of 3.38 GW at frequency 2.56 GHz with an overall efficiency of 19.3 per cent with dielectric loading. We investigated the S-band tapered MILO with partial dielectric loading and the influence of cathode misalignment on RF output power for the first time in this chapter, which has never been done before.

4.2 Introduction

The Tapered magnetically insulated line oscillator (MILO) is the crossed field high power microwave (HPM) oscillator which consists of gentle tapered slow wave structure, sharp tapered extractor section, and tapered cylindrical cathode [Eastwood *et al. 1998*]. The device is capable to produce a long pulse of up to 100 ns with power levels of several

giga-watts in GHz frequency range. The tapered MILO is just similar to the linear magnetron and operates with self-insulation condition [Eastwood *et al*., *1998* -Qiang *et al*., *2009* - Dwivedi *et al*., *2014* - Lemke *et al*., *1987*]. This self-insulation condition removes the external dc magnetic field requirement for focusing the electron beam due to which the device becomes compact. The other advantage of the self-insulation is that the device works at high voltage without any electric breakdown [Lemke *et al*., *1987*]. For electron beam generation, the device uses an explosive emission cathode which is mounted on the surface of a cylindrical cathode. The critical current which is required to get magnetic insulation is obtained by the load current generated by the load diode gap [Eastwood *et al*., *1998* -Qiang *et al*., *2009* - Dwivedi *et al*., *2014* - Lemke *et al*., *1987*]. After achieving the magnetic insulation, the electron beam flows parallel to the cathode and interacts with the normal mode of the slow wave structure of the device. Due to this beam-wave interaction, the intense electron bunches are formed in the device. MILO oscillates in its fundamental mode i.e., π mode and stores the electromagnetic energy in the form of standing wave within the gentle tapered SWS cavities [Eastwood *et al*., *1998* -Qiang *et al*., *2009* - Dwivedi *et al*., *2014*]. This stored EM energy is extracted with the help of sharp tapered extractor configuration. The sharp tapered extractor structure couples the stored EM energy with the output waveguide system of the device by changing the group velocity of the stored energy Eastwood *et al*., *1998* -Qiang *et al*., *2009*].

MILO is a very attractive and promising HPM source among all the HPM sources due to its compact size, light weight, and self-insulation property. But having all these advantages the device is suffered with low conversion efficiency and low pulse width (i.e., pulse shortening problem). To overcome these problems, a lot of design modification and studies were also reported by the researchers all over the world.

Haworth *et al*. identified some of the reasons behind the pulse shorting problem, and solved this problem to some extent by modifying the MILO structure and named this modified structure of MILO as hard tube MILO [Haworth *et al., 1998*]. In hard tube MILO, the condition of the cathode structure alignment, choke, and slow-wave structure (SWS) was modified, as result the RF output power was improved by 2.5 times as compared to the previously reported experiment [Haworth *et al., 1998*]. Fan *et al*. also reported an experimental study in which beam dump disc was used near the load side to improve the overall efficiency of the device [Fan *et al*., *2007*]. Kumar *et al.* reported a literature in which the performance of the MILO was improved by matching the impedance of different subsections of MILO [Kumar *et al., 2019*]. Xu *et al.* reported a modified MILO (i.e., ridge MILO) in which the device conversion efficiency and the frequency tenability was achieved by controlling the length of the ridge [Xu *et al., 2020*]. Improving the overall efficiency of MILO is still a major challenge for researchers around the world. In this article, with the aim of improving the efficiency of MILO, a low-loss partially dielectric filled thin MILO has been proposed.

In this chapter, the design, analytical and simulation study of the proposed structure of MILO is performed through 3D PIC simulation code CST particle studio first time. The fundamental oscillation frequency is calculated using the dispersion characteristics obtained through simulation as well as analysis.

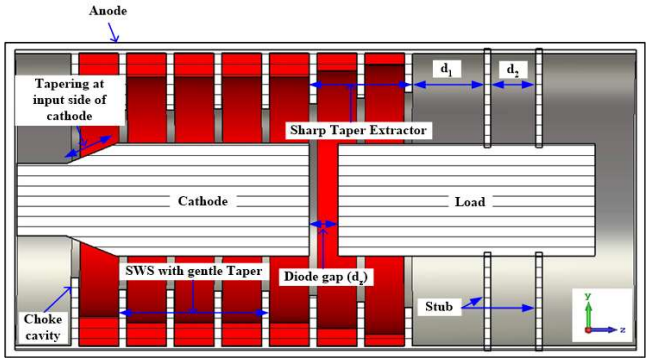

Figure 4.1. Schematic diagram of dielectric filled tapered MILO.

In addition, study of the effect of cathode misalignment on the RF output power of the MILO has been reported, that has not yet been reported for any variant of MILO anywhere. In section-II, the resonating frequency associated with the fundamental oscillation mode of a partially dielectric filled tapered interaction structure is calculated through an equivalent circuit approach. In section-III, the design parameters and electrical specification used for modelling the proposed structure is listed in Table format. In section IV, the device design parameters obtained through analysis is validated through simulation and then the modelled MILO structure is simulated to investigate the RF behaviour in the presence and absence of the dielectric loading. In addition, cathode misalignment effect is also discussed in details. Finally, the present chapter is concluded in section V.

4.3 Analysis

The schematic view of Tapered MILO structure is shown in Figure 4.1. The tapered MILO consists of axially periodic disc loaded coaxial structure in which inner cylindrical conductor is used as cathode. The cavities formed between consecutive discs in the axially periodic disc loaded coaxial structure are used as interaction structure. The cylindrical cathode is tapered at input side to match the impedance with input side. For

electron beam generation, the cylindrical surface along with side circular surface are used as explosive emission surface. A high voltage DC pulse is applied between anode and cathode at the input side which initiates the explosive emission when the electric field at the cathode reaches at threshold level. The anode section consists of gentle tapered four-cavity slow wave structure (SWS) along with one choke cavity at the input side. The extractor section consists of three extractor vanes (having inner radius more than that of the SWS vane inner radius) with sharp tapering, which helps to extract the stored RF energy [Eastwood *et al. 1998*, -Qiang *et al. 2009*]. The extractor cavities convert the standing wave into travelling wave by changing its group velocity. The interaction structure (i.e., the four gently tapered cavity SWS) is operated at π-mode. Choke cavity (i.e., first two vanes) acts as a low pass filter. This filter cavity prevents leakage of RF towards the input side i.e., DC source. At the output side four stubs (azimuthally) in two pairs (axially) (i.e., total 8 stubs) are used. The first group of stubs is kept at a distance of from the last extractor vane and second group of stubs are kept at distance from the first stub group. This configuration helps in better impedance matching with the output side. The axial distance between the cathode and the load (d_z) is a very crucial parameter for the load current and useful in self-magnetic insulation process.

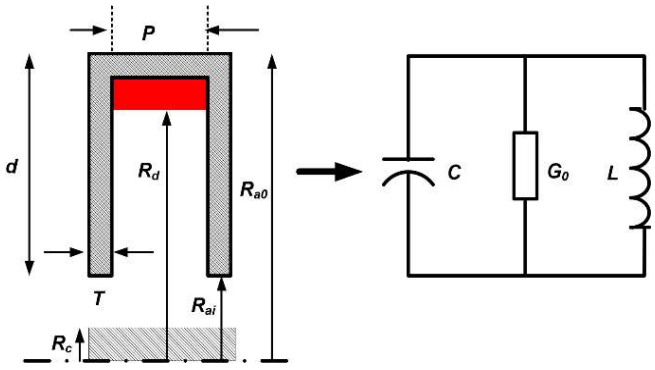

Figure 4.2: Single dielectric filled cavity and its equivalent parallel circuit of resonance system.

In the tapered MILO is shown in Figure 4.1. The interaction cavities having different cavity depth due to which it constitutes multi-cavity resonance system by electromagnetic coupling. The lowest order resonance mode also termed as fundamental mode is analyzed using equivalent circuit considering single cavity as equivalent LC circuit, shown in Figure 4.2. To increase the capacitance of the cavity, a low loss dielectric material is partially filled inside these cavities. The equivalent inductance and capacitance for a single cavity resonator which is partially filled with low loss dielectric material can be given by [Dwivedi *et al. 2014*], [Haworth *et al. 1998*], [Fan *et al. 2007*]:

$$L = \frac{\mu_0 d(P-T)}{4\pi R_{ao}} \tag{4.1}$$

$$C = 2\varepsilon_0 R_{ai} \ln\left(\frac{P+2T}{P}\right) + \frac{2\pi}{3dP}[\varepsilon_0(3R_{ao}R_d^2 - 3R_{ao}R_{ai}^2 - 2R_d^3 + 2R_{ai}^3) + \varepsilon_1(R_{ao}^3 + 2R_d^3 - 3R_{ao}R_d^2)] \tag{4.2}$$

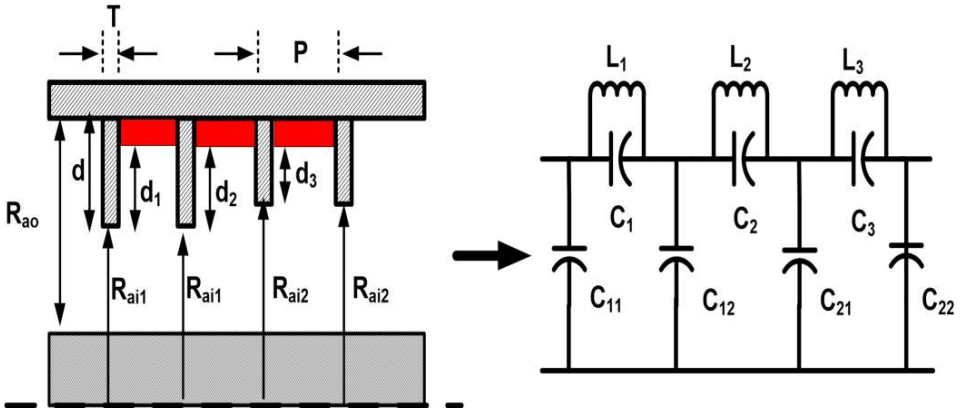

Figure 4.3: Schematic and its equivalent circuit of tapered SWS cavity with partially filled with low loss dielectric material.

Here, *'P'* is the periodicity,'d' is depth of the cavity, *'T'* is disc thickness, *'R_{ai}'* is the disc inner radius, *'R_{ao}'* is the disc outer radius, *'L'* is inductance and *'C'* is capacitance of the cavity.

The internal circuit design of the tapered slow wave structure and its equivalent circuit is shown in Fig. 4.3. For the above circuit given in Fig. 4.3, the inductance L_1, L_2, and L_3 can be calculated substituting different cavity depth d (i.e., d_1, d_2, and d_3, respectively) in Eq. (4.1). Similarly, capacitance C_1, C_2, and C_3 can be calculated by substituting different disc inner radius R_{ai} (i.e., R_{ai1}, R_{ai2}, and R_{ai3}, respectively) for different cavities in Equitation (4.2). Now, the coupling capacitance C_{11}, C_{22}, and C_{12}=C_{21} can be calculated using the expression [Dwivedi *et al.,* 2014]:

$$C_{11} = \frac{2\pi\varepsilon_0 T}{\ln(R_{ai1}/R_c)} + 8\varepsilon_0[(P-T)/2 + (R_{ai1} - 2g_1/\pi)\times\ln(\frac{\pi(P-T)+2g_1}{2g_1})] \tag{4.3}$$

$$C_{22} = \frac{2\pi\varepsilon_0 T}{\ln(R_{ai2}/R_c)} + 8\varepsilon_0[(P-T)/2 + (R_{ai2} - 2g_2/\pi)\times\ln(\frac{\pi(P-T)+2g_2}{2g_2})] \tag{4.4}$$

$$C_{12} = \frac{2\pi\varepsilon_0 T}{\ln((\mathrm{R}')/2R_c)} + 8\varepsilon_0[(P-T)/2 + ((R')/2 - (g')/\pi) * \ln(\frac{\pi(P-T)+g'}{g'})] \tag{4.5}$$

Here, R_c is the cathode radius, g_1 (=R_{ai1} - R_c), is the gap between disc inner radius and the cathode, g_2 (=R_{ai2}-R_c), g' (=g_1+g_2), R' (=R_{ai1}+R_{ai2}). The resonance frequency for the parallel resonance circuit shown in Figure 4.3 can be given calculated by:

$$\omega_{0k} = \omega_0 / \sqrt{1 + \frac{1}{4} C_{eq}\left(\frac{1}{1-\cos(\mathrm{k}\pi/\mathrm{N})}\right)} \tag{4.6}$$

where,

$$C_{eq} = \left(\frac{C_{11}}{2C_1} + \frac{C_{12}}{2C_2} + \frac{C_{21}}{2C_2} + \frac{C_{22}}{2C_3}\right)$$

Here, N is the number of resonance cavity and k (=0, 1, 2, …., 2N-1); is the different resonant modes.

4.4 Device Modelling

The device design parameters for S-band tapered MILO are calculated with the help of flow chart diagram provided in literature [Dwivedi *et al.,* 2014]. The device design parameters calculated for the frequency 2.65 GHz are listed in Table-4.1, along with the applied beam voltage, cathode radius, anode radius, SWS vane radius, dielectric radius, extractor vane radius, choke vane radius, vane thickness, periodicity and beam current.

Table 4.1: Device design specifications for dielectric filled tapered MILO [Qiang *et al.* 2009].

Particulars	**Specifications**
Voltage	500 kV
Current	35 kA
Cathode radius (R_c)	15 mm
Anode radius (R_{ao})	65 mm
SWS Vane radius (R_{ai})	45-46 mm
Dielectric radius (R_d)	43 mm
Extractor Vane radius	48, 51, 54 mm
Choke Vane radius	39 mm
Vane thickness (T)	4 mm
Periodicity (P)	24 mm
Axial diode gap (d_z)	14 mm
Stub length	49 mm

4.5 Results and discussion

In order to understand the beam-wave interaction mechanism and the ability to generate RF inside the device, simulation study has been performed. The simulation study is considered as a complimentary process to the experiments by which one can get an overall idea about how the device generates RF wave at desired frequency and desired power. To validate the design parameters listed in Table 4.1, the dispersion characteristic is plotted with the help of Eq. (4.6) which is obtained via analytical calculations. From the dispersion characteristic we can easily calculate the resonance frequency associated with the desired mode (in this case it is π-mode) of the device.

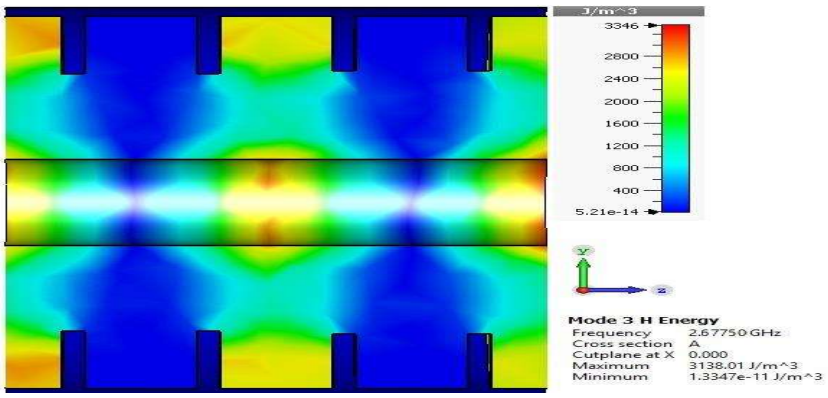

Figure 4.4: Magnetic field contour plot of the SWS structure in π-mode oscillation at 2.6775 GHz.

Now, the structure is modelled with the help of the design parameters listed in Table 4.1 and simulated it in a beam absent (cold) environment. The EIGENMODE solver provides the electric field distribution and resonating frequency associated with the different resonating mode which is noted and used to verify the analytical result. Figure 4.4 shows the field pattern (contour plot) inside the structure obtained through the cold simulation. The contour plot shows that SWS cavities oscillate in its fundamental π-mode

and resonating frequency is 2.67 GHz. From Figure 4.5, (analytically obtaineddispersion characteristic) the resonating frequency associated with the π-mode is 2.58 GHz which shows the close agreement with the simulated results.

In Figure 4.5 the dispersion diagram obtained through analytically and through simulation is presented. From the figure 4.5 it is noticed that the fundamental resonating frequency of the device is 2.67 GHz for interaction cavity without dielectric filling and 2.58 GHz for the interaction cavity with dielectric ($\varepsilon_r = 4$) filling inside the cavities. From Figure 4.4 and 4.5, it can be concluded that the operating frequency obtained through analysis and simulation are in close agreement of ~3%. The decrease in the frequency is noted in dispersion diagram because due to the dielectric loading within the cavities. The dielectric loading mainly increases the effective equivalent capacitance which cause decrease in the operating frequency. To maintain magnetic insulation the critical current must be achieved by axial diode formed between anode and cathode. Some minimum distance between anode-cathode (diode gap d_z) forms axial diode which is responsible for the critical current required for magnetic insulation [Eastwood *et al.,* 1998]. The diode gap d_z is an important parameter to control diode current and beam wave interaction. Larger diode gap leads low diode current for magnetic insulation and smaller diode gap leads large diode current which results in weaker beam-wave interaction. After magnetic insulation the electron sheath confine between the tip of the disc and cathode along the z-direction [Creedon *et al.,* 1977]. The slow wave structure of MILO comprises gentle tapered of the coaxial discs, forming resonant cavities.

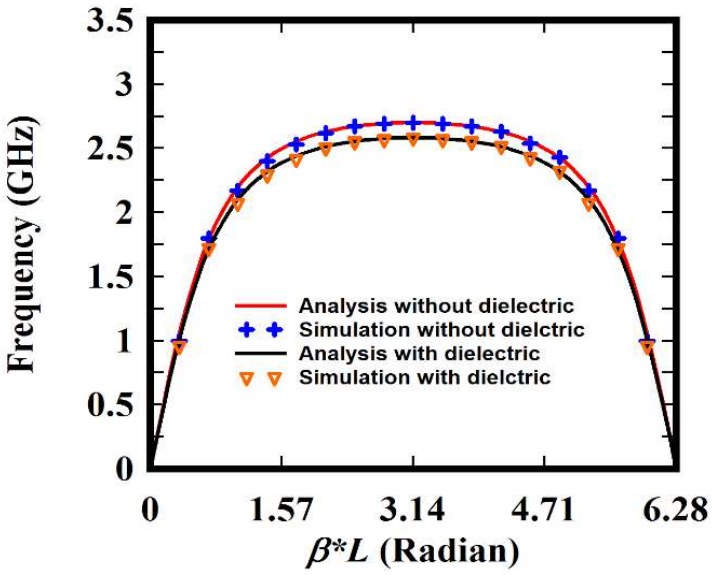

Figure 4.5: Dispersion relation of tapered slow wave structure with and without dielectric filling inside cavities.

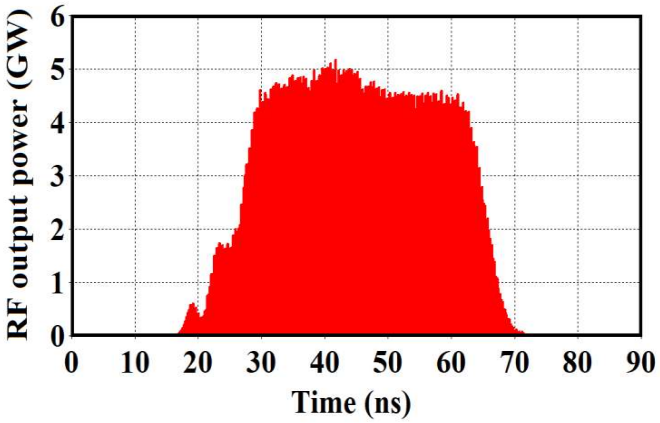

Figure 4.6: Temporal RF output peak power obtained at the output port of the device without dielectric loading inside the cavities.

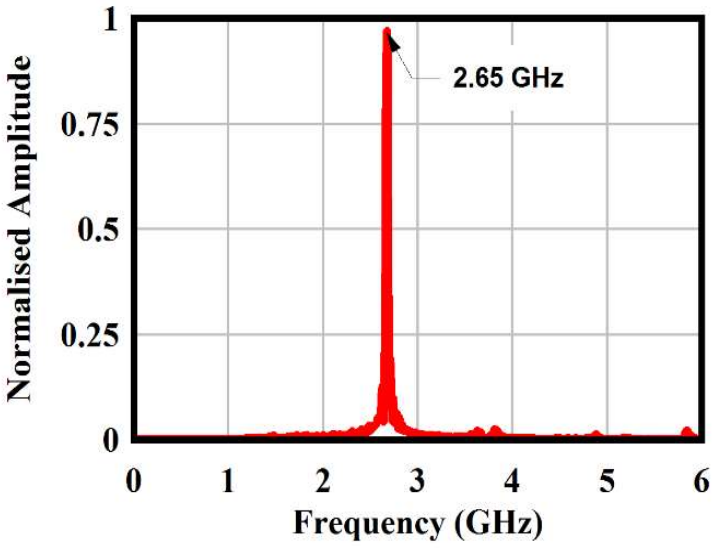

Figure 4.7: FFT of RF signal obtained at output port without dielectric loading inside the cavities.

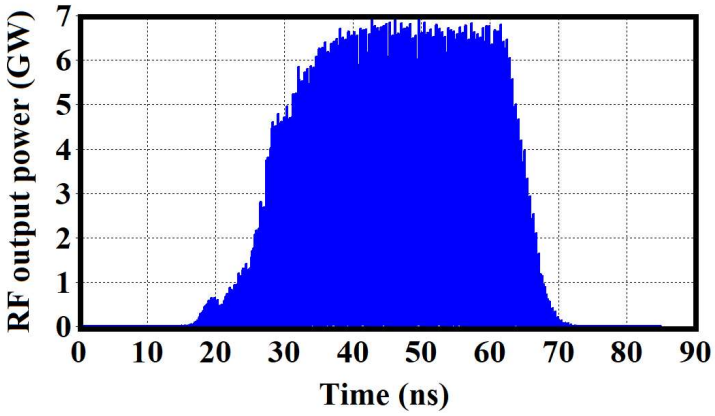

Figure 4.8: Temporal RF output peak power obtained at the output port of the device with dielectric ($\varepsilon_r = 4$) loading inside the cavities.

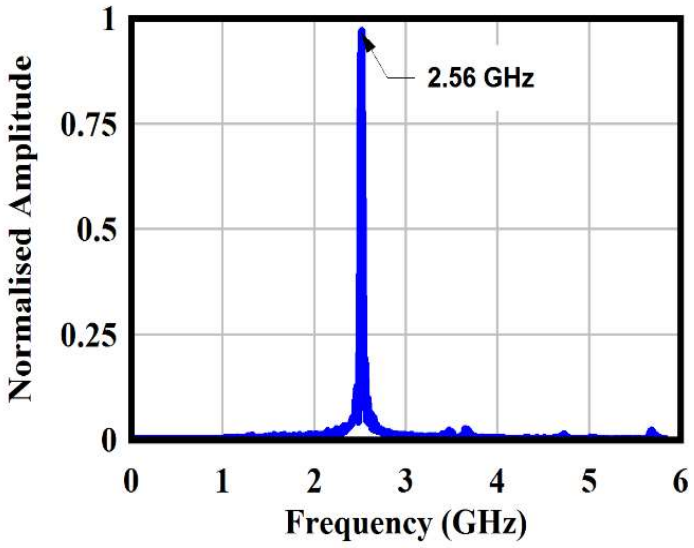

Figure 4.9: FFT of RF signal obtained at output port with dielectric ($\varepsilon_r = 4$) loading inside the cavities.

Tapering provides power flow with amplification through beam-wave interaction supported by SWS [Eastwood *et al.,* 1998]. The magnetically insulated electron sheath induces noise and generates oscillation when drift velocity of electrons become equal to phase velocity supported by SWS cavities. The axial electron motion permits the excitation of resonant TM_{01} mode. These oscillation forms standing wave inside SWS cavities with identical frequencies, which are spaced symmetrically with respect to π-mode. These oscillations are amplified by the beam-wave interaction process. Thus, energy is stored inside the cavities in form of standing wave. The extractor section is used to extract this stored energy by changing standing wave into travelling wave. The sharp tapering provided to the extractor discs inner radius to extract the power via matching impedance wall boundary condition at coaxial line section towards output [Eastwood *et al.,* 1998]. The load is supported with stub which is about $\lambda_g / 4$ distance from last extractor disc [Qiang *et al.,* 2009].

The beam present simulation (i.e., hot simulation) is carried out for the RF performance estimations (i.e., RF output power and efficiency) of the tapered MILO with and without dielectric filling within cavities. PIC simulation code 'CST Particle studio' is used for the beam present simulation. A high voltage DC pulse is applied between cathode and anode which causes electrons emission from the cylindrical cathode surface. Emitted electrons initially move radially upward i.e., towards the slow wave structure. To study the performance of partially dielectric filled tapered MILO, PIC simulation of the reported tapered MILO given in literature has been carried out first (i.e., without any dielectric loading) and then with dielectric loading. The beam present (hot) simulation is performed with the applied beam voltage and beam current (i.e., 500 kV diode voltage and 35 kA diode current). The obtained simulation results are then compared with the reported experimental results available in the literature [Qiang *et al. 2009*]. After that, to study the effect of dielectric filling inside the interaction structure, the modelled structure is simulated and obtained results are compared with the previously obtained result. Figure 4.6 shows the temporal RF output peak power at the output port of the device without dielectric loading inside the cavities. It can be seen from Figure 4.6 that the peak RF power generated by the device after applying 500 kV of input voltage and 35 kA of input current is 4.8 GW and the average power is 2.4 GW which is equal to the average RF power reported in the literature [Qiang *et al. 2009*] which also validates the device design. The electronic efficiency of the device is approx. 14% through PIC simulation and in close agreement with the reported experimental results within ~3%. Figure 4.7 shows the frequency spectrum of RF signal at output port without dielectric loading inside the cavities. The sharp peak in Figure 4.7 is corresponding to the resonating frequency which is 2.65 GHz and confirms the excitation of desired TM_{01} mode that was obtained from the Eigenmode simulation

(Figure 4.4) (cold cavity simulation) and it is nearly equal. Now the modelled structure is modified by inserting the dielectric material inside the cavities and simulated again. Considering the same electric parameters (i.e., 500 kV voltage and 35 kA current), the obtained peak RF output power is shown in Figure 4.8. It can be observed from the figure is that the Peak RF output power is around 6.8 GW and average power is around 3.38 GW with dielectric ($\varepsilon_r = 4$) loading inside the cavities. Thus, the overall efficiency obtained through the device is around 19.3 % which shows improvement in the performance of the device. Figure 4.9 shows the Fast Fourier Transform (FFT) of RF signal obtained at output port with dielectric ($\varepsilon_r = 4$). It can be observed from that the operating frequency of the device is around 2.56 GHz which is decreases below ~1%. This decrease in the operating frequency is observed due to beam loading effect.

4.5.1 Cathode Misalignment Effect

Cathode misalignment studies are carried out to investigate the performance dependency of the device with the azimuthal symmetry of the structure. To observe this effect, ~5% misalignment of cathode with its axis has deliberately introduced inside the device. The PIC simulation studies show that due to this misalignment, asymmetric beam wave interactions take place and some unwanted modes are generated inside the device. Figure 4.10 shows the two different modes are generated in which one degenerative mode (i.e., TE_{11} mode) while other is desired mode (i.e., and TM_{01} mode) and both modes try to dominant over each other modes. The RF power distribution associated with these modes are shown in Figure 4.11.

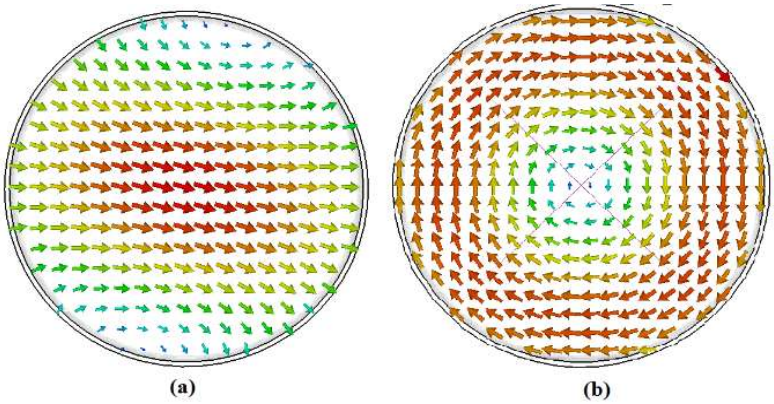

Figure 4.10: Different modes excited inside the device due to cathode misalignment, **(a)** degenerative TE_{11} mode **(b)** desired TM_{01} mode.

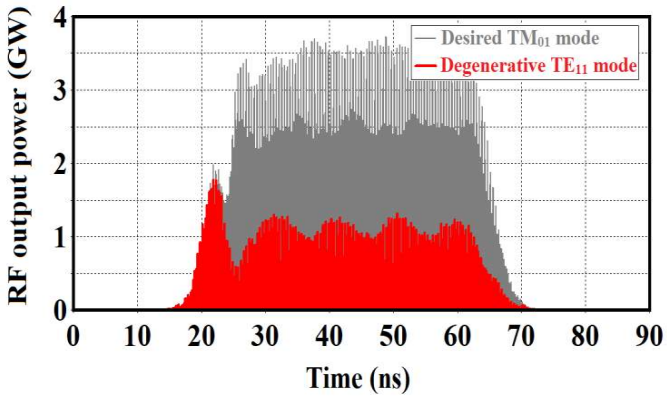

Figure 4.11: Temporal RF output peak power obtained at the output port of the device with dielectric ($\varepsilon_r = 4$) loading inside the cavities and cathode axis misalignment with 5%.

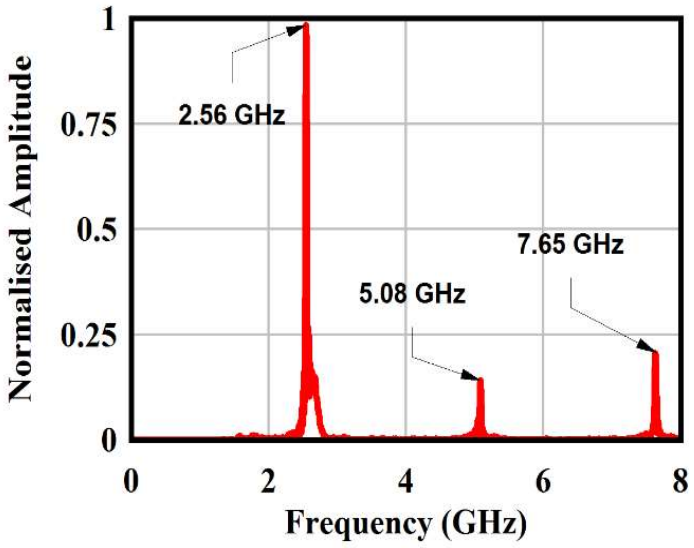

Figure 4.12: FFT of RF signal obtained at output port with dielectric ($\varepsilon_r = 4$) loading inside the cavities after ~5% cathode misalignment.

From the Figure 4.11, it can be seen that the peak RF power distributed in desired mode (i.e., TM_{01} mode) is 3.5 GW (or 1.75 GW of average RF power) while in undesired mode (i.e., TE_{11} mode) is about 1 GW (or 0.5 GW of average RF power). In addition to these two modes, RF power are also distributed between other unwanted modes whose amplitude is smaller than that of the TE_{11} and TM_{01} modes. Therefore, from this simulation study it can be concluded that a very small cathode misalignment (i.e., ~5%) with axis decreases the average RF power approximately by 50%. The FFT of the RF signal obtained after cathode misalignment is shown in Figure 4.12. The figure shows that the desired mode as well as other modes and harmonics of the desired mode are generated inside the device which is mainly responsible for the degradation of RF power and efficiency of the device. For better visualization, all obtained results are compared with experimental results, and the whole work is briefly listed in Table 4.2.

Table 4.2: Comparison of device performance with published and present simulation

Particulars	**Tapered MILO [2]**	**Present Result Tapered MILO (Without Dielectric Loading)**	**Present Result Tapered MILO (With Dielectric Loading)**
Voltage	500 kV	500 kV	500 kV
Current	35 kA	35 kA	35 kA
Output RF pulse width	25 ns	45 ns	45 ns
Output RF Power (Average)	2.5 GW	2.4 GW	3.38 GW
Operating Frequency	2.65 GHz	2.65 GHz	2.56 GHz
Overall Efficiency	14.00 %	13.71 %	19.30 %
Cathode Misalignment Study	Not Reported	Presented	Presented

4.6 Conclusion

In this chapter, the proposed S-band dielectric filled tapered MILO was studied in detail through analysis and using commercial PIC simulation code 'CST Particle Studio'. The equivalent circuit analysis was performed to obtained the equivalent capacitance, equivalent inductance and coupling capacitance of the dielectric filled interaction structure. Further, the expression for the dispersion characteristics was derived for the fundamental resonating mode associated with the interaction structure. The tapered MILO designed parameter was also verified by both i.e., analysis and simulation.

The device performance was obtained for the typically selected beam parameters. The device generates an average power of ~2.4 GW with and electronic efficiency of ~13.71% without dielectric loading. Further, with dielectric loading the device generates an average power of 3.38 GW at frequency 2.56 GHz and the obtained overall efficiency of 19.3%. In addition, studies were reported on the effect of cathode misalignment on the generated RF output power of MILO, which had not yet been reported anywhere. Finally, this research work suggests that the overall efficiency of any HPM system can be improved using this approach.